Modeling and Predicting Land Use/Land Cover Dynamics in Shahrekord (1990–2030) Using a Comparative CA-Markov and LCM Models

Faraz Sarhadi [1], Hamed Hosein Amini [1]

[1] Department of Surveying and Geoinformatics Engineering, College of Engineering, University of Tehran, Tehran, Iran – sarhadifaraz@gmail.com; amini79hamed@gmail.com

Keywords: LULC, Change Modeling, CA-Markov, Land Change Modeler (LCM), Shahrekord, Landsat.

Abstract

Accurate prediction of land-use/land-cover (LULC) change is essential for sustainable urban and environmental planning. This study analyzes and models multi-decadal LULC dynamics in Shahrekord, Iran, using Landsat Surface Reflectance images for 1990, 2000, 2009, 2020, and 2024. Four classes were identified: Built-up/Barren (UB), Agriculture (AG), Water (WT), and Vegetation/Orchards (VG). LULC maps were produced using the Maximum Likelihood Classification (MLC) method in ArcGIS, based on pre-processed data from Google Earth Engine (GEE).Two predictive approaches were compared in TerrSet: Cellular Automata–Markov (CA-Markov) and Land Change Modeler (LCM) with a multilayer perceptron (MLP). Model performance was evaluated using hindcasts for 2020 and 2024, applying Overall Accuracy (OA), Kappa, and Pontius metrics. The CA-Markov model achieved higher accuracy and was therefore selected to predict LULC for 2030.Between 1990 and 2024, the UB class remained dominant, while AG increased in certain periods; WT and VG showed minor fluctuations. The findings confirm that neighborhood-based transitions drive most changes, enabling reliable short-term projections. The main limitations are the merged UB class and irregular time intervals. Recommendations for class refinement and temporal standardization are provided to improve future modeling and reproducibility.

1.Introduction

Land-use and land-cover (LULC) change is both a primary driver and a key indicator of global environmental transformation, reflecting the complex interactions between human activities and the natural environment. The dynamics of LULC have significant implications for a wide range of global challenges, including sustainable development, climate regulation, food security, biodiversity conservation, and urban growth management. Therefore, monitoring historical patterns and accurately predicting future scenarios have become essential for developing proactive and evidence-based land management strategies.The advancement of Earth Observation (EO) technologies, particularly Remote Sensing (RS), has revolutionized the study of LULC dynamics. Satellite missions such as the Landsat series provide a unique, long-term archive of Earth's surface conditions, enabling consistent multi-decadal analyses at various spatial and temporal scales. When integrated with Geographic Information Systems (GIS), these data offer a robust analytical framework for processing, classifying, and visualizing spatial patterns and trends in land cover. Among the many classification techniques, the Maximum Likelihood Classification (MLC) algorithm remains one of the most reliable and statistically rigorous approaches, known for its effectiveness in handling multi-spectral datasets across diverse landscapes.In recent years, LULC research has shifted beyond retrospective monitoring toward the prediction of future trajectories. Anticipating land-use dynamics is crucial for assessing potential environmental consequences, evaluating alternative policy scenarios, and promoting sustainable spatial planning. To achieve this, various predictive models have been developed, among which the Cellular Automata–Markov (CA-Markov) model and the Land Change Modeler (LCM) are among the most widely applied. The CA-Markov model integrates the probabilistic forecasting capabilities of Markov chains with the spatial simulation power of Cellular Automata, while the LCM employs empirical and machine-learning techniques—such as the Multi-Layer Perceptron (MLP)—to capture complex, non-linear transition behaviors driven by environmental and socio-economic factors.

Numerous studies worldwide have demonstrated the utility of these models for simulating LULC change. For instance, Ait El Haj et al. (2023) compared CA-Markov and LCM models in Morocco's Lakhdar sub-basin and found the CA-Markov model achieved higher accuracy. Similarly, Wang et al. (2021) applied the CA-Markov model in Thimphu, Bhutan, to simulate urban expansion in a high-altitude city, while Aburas et al. (2018) conducted a comparative analysis in Seremban, Malaysia, confirming that model performance is region-specific and requires local validation.Building on this foundation, the present study provides a comprehensive analysis of LULC dynamics in Shahrekord, Iran, over a 34-year period (1990–2024), with a forward-looking projection to 2030. The study's main contribution lies in its integrated methodological framework, combining the cloud-computing capabilities of Google Earth Engine (GEE) for efficient image acquisition and pre-processing, ArcGIS for robust supervised classification using MLC, custom Python scripts for transparent and replicable accuracy assessment, and the TerrSet environment for a rigorous comparative evaluation of the CA-Markov and LCM-MLP models. Through this seamless and multi-platform workflow, the study not only delivers a reliable projection for the future of Shahrekord but also provides a replicable and adaptable framework for analyzing LULC dynamics in other rapidly urbanizing semi-arid regions.

2.Study Area

The study area is centered on Shahrekord, the capital city of Chaharmahal and Bakhtiari Province, situated in the mountainous western region of Iran. To capture both the dynamics of urban expansion and its interaction with the surrounding landscape, the study area was delineated as a 15-kilometer buffer zone around the city center. Geographically, it extends approximately between latitudes 32.19°N–32.50°N and

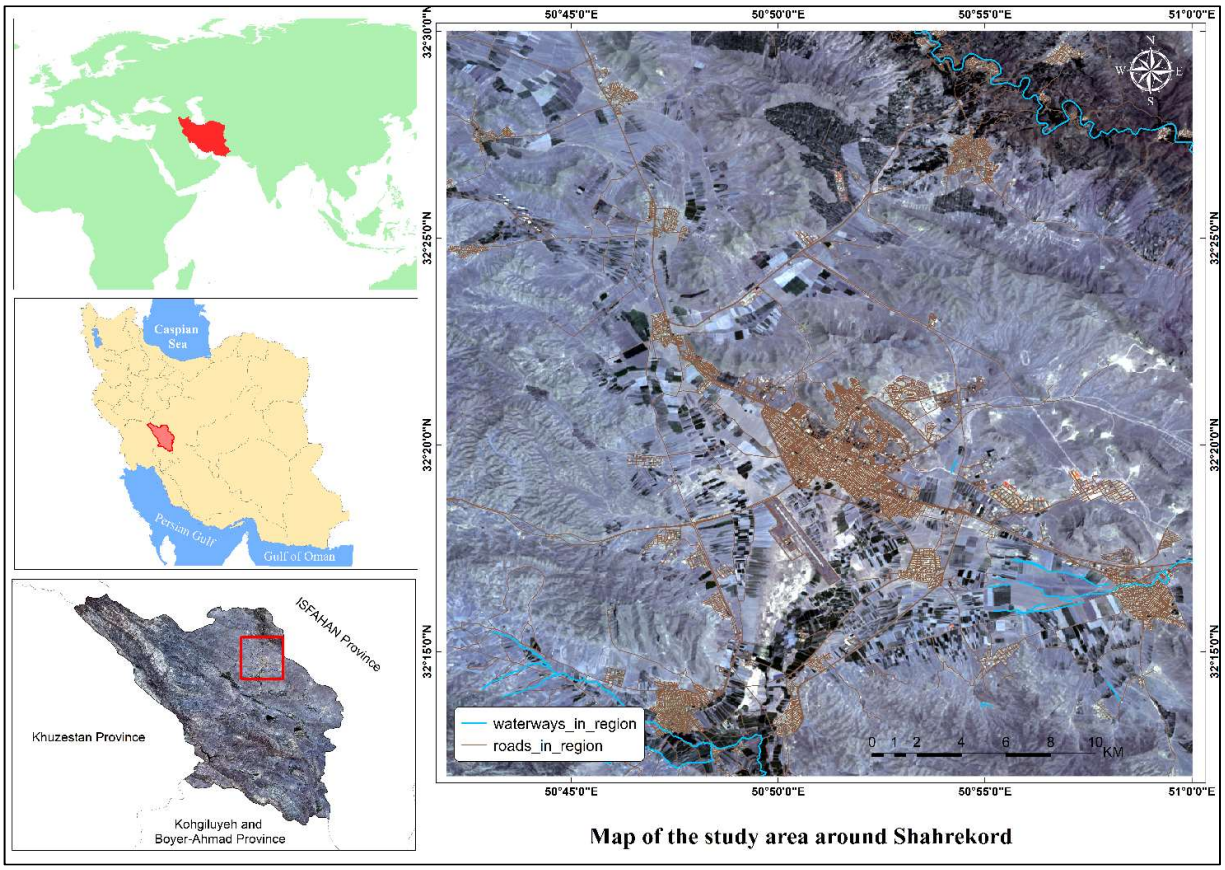

Figure 1. Study area location map of Shahrekord, Iran.

longitudes 50.70°E–51.00°E (Figure 1). Shahrekord is characterized by its high elevation, averaging about 2,070 m above sea level, which makes it one of the highest provincial capitals in Iran. The topography includes relatively flat plains where most of the city lies, surrounded by foothills that influence land-use patterns and hydrological processes. The climate is classified as cool semi-arid (Köppen: BSk), with cold, often snowy winters and mild, dry summers. Annual precipitation is limited, and for image selection, Landsat scenes with less than 10 % cloud cover were used to ensure optimal visibility.As the primary administrative and economic center of the province, Shahrekord has undergone continuous population growth and urban expansion over the past few decades. This development has placed increasing pressure on nearby lands, resulting in noticeable conversions of agricultural and vegetated areas into built-up zones. The landscape comprises a mosaic of four primary LULC classes—Built-up/Barren (UB), Agriculture (AG), Water (WT), and Vegetation/Orchards (VG)—that were analyzed throughout this study. The combination of its distinct climate, diverse topography, and documented urban growth makes Shahrekord an ideal case study for analyzing multi-decadal LULC transitions and modeling future development scenarios.

3.Data and Materials

This section describes the satellite datasets and software tools used for land-use/land-cover (LULC) mapping, change detection, and modeling.

3.1. Satellite Data and Pre-processing

The primary data for this research consist of a multi-temporal image series from the Landsat program, used to cover the study's time frame from 1990 to 2024. The specifics of these data are as follows:

- **Sensors:** LULC maps for the years 1990, 2000, and 2009 were derived from Landsat 5 Thematic Mapper (TM) imagery. For the years 2020 and 2024, images from the Landsat 8 Operational Land Imager (OLI) sensor were utilized.
- **Source and Pre-processing:** All imagery was sourced and processed via the Google Earth Engine (GEE) cloud-computing platform. The use of GEE provided access to Landsat's Analysis-Ready Data (ARD), specifically the Surface Reflectance (SR) products, which are pre-corrected for atmospheric and geometric distortions. This approach streamlined the workflow, eliminated the need for manual corrections, and ensured radiometric consistency across the time series.
- **Image Selection Criteria:** To minimize the effects of seasonal phenological variations on vegetation and ensure data consistency, images were selected from the growing season (late spring to late summer). Furthermore, the image collection for each target year was filtered to include only scenes with less than 10% cloud cover over the study area. Finally, a median composite image was generated for each year from the filtered collection to minimize the impact of residual clouds, shadows, and other potential artifacts.

The details of the satellite imagery used in this study are summarized in the table below:

Year	Satellite/Sensor	GEE Collection ID	Spatial Resolution
1990	Landsat 5 / TM	LANDSAT/LT05/C02/T1_SR	30 m
2000	Landsat 5 / TM	LANDSAT/LT05/C02/T1_SR	30 m
2009	Landsat 5 / TM	LANDSAT/LT05/C02/T1_SR	30 m
2020	Landsat 8 / OLI	LANDSAT/LC08/C02/T1_SR	30 m
2024	Landsat 8 / OLI	LANDSAT/LC08/C02/T1_SR	30 m

Table 1. Characteristics of the Landsat imagery used in this study

3.2. Software and Tools

The research workflow was implemented using an integrated suite of geospatial software and tools:

- Google Earth Engine (GEE): Used for searching, acquiring, filtering, and pre-processing the Landsat satellite imagery.
- ArcGIS 10.8**:** Employed for conducting the supervised classification using the Maximum Likelihood (MLC) algorithm, post-processing the classified maps (e.g., applying a majority filter), and producing the final cartographic outputs.
- TerrSet Geospatial Modeling System (IDRISI): This served as the primary tool for LULC change modeling. Specifically, the CA-Markov module was used for stochastic simulation based on Markov chains, and the Land Change Modeler (LCM) was employed for empirical modeling and a comparative analysis.
- Python (with GDAL and NumPy libraries): Utilized for developing custom scripts to automatically and replicably calculate the confusion matrix and derive quantitative accuracy assessment metrics, including Overall Accuracy and the Kappa Coefficient.

4.Methods

The methodological framework of this study integrates multiple platforms and techniques to conduct a multi-decadal analysis and prediction of land-use/land-cover (LULC) changes. As illustrated in Figure 2, the overall workflow consists of three primary stages: data acquisition and pre-processing, LULC classification with corresponding accuracy assessment, and predictive modeling followed by validation, which ultimately leads to the generation of the projected LULC map for the year 2030.

4.1 Data Acquisition and Characteristics

A multi-temporal dataset of Landsat imagery was acquired through the Google Earth Engine (GEE) platform, which provides direct access to the complete Landsat archive and enables cloud-based pre-processing. To maintain temporal consistency and capture vegetation phenology, images were selected from the growing season (late spring to late summer) with less than 10 % cloud cover. The dataset comprises images from the Landsat 5 Thematic Mapper (TM) and Landsat 8 Operational Land Imager (OLI) sensors, corresponding to the years 1990, 2000, 2009, 2020, and 2024. All images were reprojected to a common spatial reference system (UTM Zone 39 N, WGS 84) to ensure geometric consistency across the time series. The characteristics of these datasets are summarized in Table 1.

4.2 LULC Classification and Accuracy Assessment

The classification process was carried out in ArcGIS 10.8 using the Maximum Likelihood Classification (MLC) algorithm. For each target year, a set of training samples was manually digitized through visual interpretation of high-resolution imagery and local ground-truth knowledge. These samples represented four LULC classes defined for the study area: Built-up/Barren (UB), Agriculture (AG), Water (WT), and Vegetation/Orchards (VG). The spectral properties of these samples were used to generate signature files, which served as input for the MLC classifier. As a parametric approach, MLC assigns each pixel to the class with the highest probability of membership based on the multivariate normal distribution of spectral values. for each year. The Extract Values to Points tool was used to compare classified pixel values against reference data. A confusion matrix was then produced, and key accuracy metrics—Overall Accuracy (OA), Producer's Accuracy (PA), User's Accuracy (UA), and the Kappa Coefficient (κ)—were calculated using custom Python scripts developed with the GDAL and NumPy libraries. These metrics

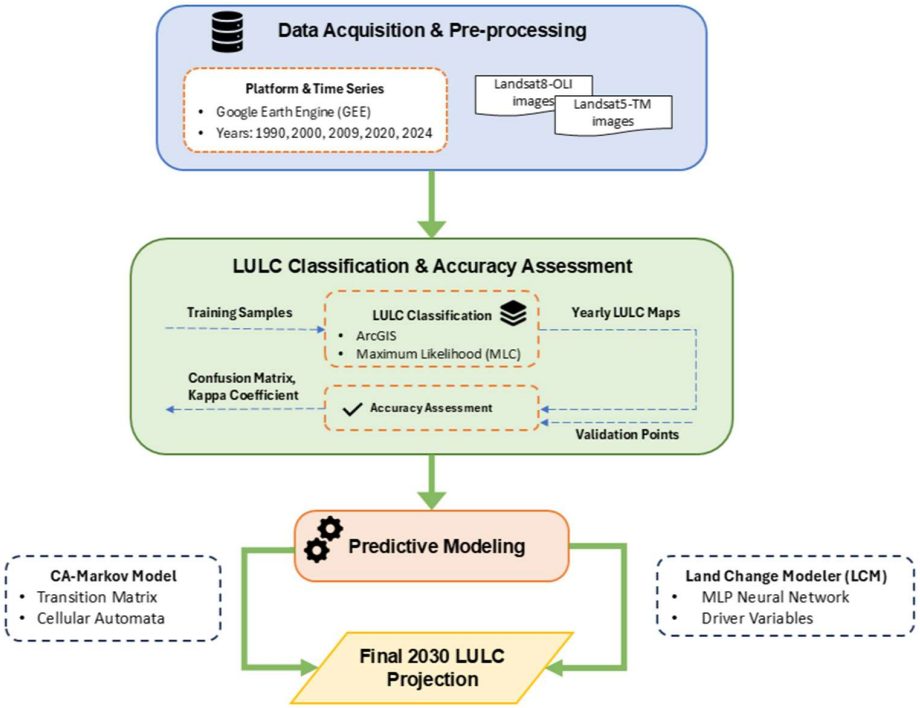

Figure2. Flowchart of the adopted methodology

This contribution has been peer-reviewed. The double-blind peer-review was conducted on the basis of the full paper.
https://doi.org/10.5194/isprs-annals-X-4-W8-2025-675-2026 | © Author(s) 2026. CC BY 4.0 License.

provided a consistent, quantitative basis for assessing thematic accuracy across all classified maps.

4.3 Predictive Modeling and Validation Framework

The prediction of future land-use/land-cover (LULC) dynamics was carried out using two modeling approaches within the TerrSet Geospatial Monitoring and Modeling System (IDRISI): the Cellular Automata–Markov (CA-Markov) model and the Land Change Modeler (LCM). These models were selected because they represent two complementary paradigms—probabilistic and empirical—allowing a comprehensive comparison of predictive performance for the Shahrekord landscape. In the CA-Markov model, the Markov chain component quantifies transition probabilities between LULC classes based on observed changes during historical periods (e.g., 1990–2000, 2000–2009, 2009–2020). These probabilities describe the likelihood of each pixel transitioning from one class to another over a given time interval. The Cellular Automata (CA) component then spatially allocates these transitions using neighborhood rules that simulate the spatial contiguity and diffusion patterns characteristic of urban and environmental processes. A 5×5 Moore neighborhood was applied, and the number of simulation iterations was adjusted to align with the temporal interval between calibration and target years. The Land Change Modeler (LCM), by contrast, applies a Multi-Layer Perceptron (MLP) neural network to estimate transition potentials. Predictor variables (drivers) such as elevation, slope, aspect, distance to roads, distance to water, and distance to built-up areas were used to represent physical and anthropogenic factors influencing LULC change. The MLP was trained on observed transitions from earlier time periods, and the resulting transition potential maps were used to simulate future LULC distributions.Model validation was performed through a hindcasting approach, in which maps from earlier years were used to simulate a subsequent year with known ground truth (e.g., simulating 2020 based on 2000–2009 transitions, and simulating 2024 based on 2009–2020 transitions). The simulated maps were then compared with the corresponding classified maps using cross-tabulation and agreement metrics such as Overall Accuracy (OA), Kappa (κ), and Pontius family indices (*Kno*, *Klocation*, *Kstandard*). These metrics provided an objective measure of the spatial and categorical agreement between simulated and reference maps. Based on the validation results, the model with the higher agreement—CA-Markov—was selected to project the LULC map for **2030**. This model's superior performance suggests that transition probabilities combined with spatial neighborhood effects provide a more realistic representation of change dynamics in Shahrekord's semi-arid environment.

5.Results

This section presents the main findings of the study, beginning with the accuracy assessment of the historical land-use/land-cover (LULC) classifications, followed by an analysis of spatio-temporal dynamics between 1990 and 2024, and concluding with the comparative performance evaluation of the predictive models.

5.1 Accuracy of LULC Classifications

The thematic accuracy assessment of the classified LULC maps, evaluated using independent validation points, demonstrates a substantial improvement over time, confirming the reliability of the base maps for change detection and modeling. As summarized in Table 2, the Overall Accuracy (OA) increased from 53.4% for the 1990 classification to 88.4% for 2024, while the Kappa Coefficient (κ) improved from 0.382 (fair agreement) to 0.836 (strong agreement).The relatively low accuracy in 1990 is primarily attributed to the lower spectral and radiometric quality of the earlier Landsat TM sensor data. However, from 2000 onwards, the classification accuracy remained consistently high, providing a robust foundation for subsequent modeling. The Built-up/Barren (UB) class was classified with particularly high precision across all years, especially in later periods, while moderate confusion occurred between Agriculture (AG) and Vegetation/Orchards (VG) classes—mainly due to their similar spectral characteristics during the growing season.

Metric	1990	2000	2009	2020	2024
Overal Accuracy	53.4%	85.1%	83.1%	83.5%	88.4%
Kappa Coefficient	0.382	0.790	0.764	0.771	0.836
Per-class Accuracy (UA/PA)					
Urban/Bare (0)	0.52/1.00	1.00/0.90	1.00/0.96	1.00/0.97	1.00/0.91
Agriculture (1)	0.45/0.26	1.00/0.78	0.76/0.80	0.86/0.78	0.87/0.90
Water (2)	0.50/0.62	0.65/0.73	0.88/0.78	0.71/0.45	0.75/0.75
Vegetation (3)	0.67/0.44	0.67/0.93	0.62/0.67	0.64/0.93	0.80/0.92

Table 2. Accuracy assessment results for the classified LULC maps from 1990 to 2024, including Overall Accuracy (OA), Kappa Coefficient, User's Accuracy (UA), and Producer's Accuracy (PA).

5.1 Spatio-Temporal LULC Dynamics (1990-2024)

This section examines the spatial and temporal dynamics of land-use/land-cover (LULC) change in Shahrekord over a 34-year period. Understanding these trends is crucial for identifying patterns of urban growth, agricultural expansion, and environmental transformation under semi-arid conditions. By analyzing multi-temporal classified maps, statistical summaries, and transition matrices, this section highlights both the magnitude and direction of LULC transitions that shaped the region's landscape. As shown in Tables 3, 4, and 5, the Built-up/Barren (UB) class remained dominant (87.8% in 1990) but declined intermittently—most notably during 2000–2009—while Agriculture (AG) expanded, peaking at 14.1% in 2009 and stabilizing near 14.0% in 2024. Water (WT) and Vegetation/Orchards (VG) occupied smaller, fluctuating shares; WT increased sharply in 2000 (3.67%) and then stabilized, while VG declined steadily due to urban and agricultural pressures. Accuracy metrics in Table 4 confirm the consistency of these results, and Table 5 shows high persistence in UB and AG with frequent AG↔VG transitions driven by seasonal or irrigation variability. The gain–loss analysis in Figure 3 further illustrates these trends. Between 1990 and 2009, AG and VG gained area at the expense of barren lands, while 2009–2020 marked moderate urban growth and notable agricultural and vegetation loss. The 2024–2030 projection indicates limited UB expansion with moderate AG and VG recovery. Overall, these findings reveal a gradual shift toward a human-dominated mosaic, shaped mainly by urbanization and agricultural intensification across Shahrekord's semi-arid landscape.

	1990		2000		2009		2020		2024	
	Producer's accuracy(%)	User's accuracy(%)	Producer's accuracy(%)	User's accuracy(%)	Producer's accuracy(%)	User's accuracy(%)	Producer's accuracy(%)	User's accuracy(%)	Producer's accuracy(%)	User's accuracy(%)
Bareland-Urban	69.77	100.00	100.00	92.31	100.00	96.67	94.44	97.14	100.00	90.62
Agriculture	59.09	43.33	88.46	76.67	73.53	83.33	79.41	77.14	76.47	86.67
Water	89.29	83.33	84.00	70.00	84.62	73.33	94.74	51.43	95.65	73.33
Vegetation	70.37	63.33	69.05	96.67	61.29	63.33	62.75	91.43	75.00	90.00
Overall Accuracy(%)	**72.50%**		**84.50%**		**79.17%**		**79.29**		**85.25%**	
Kappa coefficient	**0.6333**		**0.7927**		**0.7222**		**0.7238**		**0.8033**	

Table 3. LULC area statistics from 1990 to 2024.

	1990		2000		2009		2020		2024	
	Producer's accuracy(%)	User's accuracy(%)	Producer's accuracy(%)	User's accuracy(%)	Producer's accuracy(%)	User's accuracy(%)	Producer's accuracy(%)	User's accuracy(%)	Producer's accuracy(%)	User's accuracy(%)
Bareland-Urban	69.77	100.00	100.00	92.31	100.00	96.67	94.44	97.14	100.00	90.62
Agriculture	59.09	43.33	88.46	76.67	73.53	83.33	79.41	77.14	76.47	86.67
Water	89.29	83.33	84.00	70.00	84.62	73.33	94.74	51.43	95.65	73.33
Vegetation	70.37	63.33	69.05	96.67	61.29	63.33	62.75	91.43	75.00	90.00
Overall Accuracy(%)	**72.50%**		**84.50%**		**79.17%**		**79.29**		**85.25%**	
Kappa coefficient	**0.6333**		**0.7927**		**0.7222**		**0.7238**		**0.8033**	

Table 4. Classification accuracy of LULC maps (1990–2024).

		Markov Chain Model				LCM Model			
		Bareland-Urban	Agriculture	Water	Vegetation	Bareland-Urban	Agriculture	Water	Vegetation
1990-2000	**Bareland-Urban**	**0.9347**	0.0376	0.0244	0.0033	0.**9403**	0.0349	0.0221	0.0027
	Agriculture	0.4606	**0.3784**	0.0946	0.0663	0.4265	0.**4215**	0.0892	0.0629
	Water	0.0242	0.0203	**0.6870**	0.2685	0.0131	0.0160	**0.7175**	0.2534
	Vegetation	0.5224	0.2507	0.1207	**0.1062**	0.4869	0.2434	0.1127	**0.1569**
2000-2009	**Bareland-Urban**	**0.9008**	0.0890	0.0020	0.0082	**0.8842**	0.1025	0.0025	0.0108
	Agriculture	0.2300	**0.6550**	0.0139	0.1011	0.2665	**0.6133**	0.0162	0.1040
	Water	0.4763	0.2847	**0.1564**	0.0826	0.5018	0.2937	**0.1222**	0.0823
	Vegetation	0.1020	0.4284	0.0925	**0.3771**	0.1434	0.4453	0.0832	**0.3281**
2009-2020	**Bareland-Urban**	**0.9419**	0.0519	0.0015	0.0047	**0.9456**	0.0486	0.0013	0.0044
	Agriculture	0.5789	**0.3547**	0.0297	0.0367	0.5420	**0.3944**	0.0283	0.0353
	Water	0.2689	0.2105	**0.3588**	0.1618	0.2446	0.1998	**0.3992**	0.1563
	Vegetation	0.2415	0.3941	0.0957	**0.2687**	0.2152	0.3803	0.0904	**0.3140**
2020-2024	**Bareland-Urban**	**0.9359**	0.0625	0.0007	0.0009	0.9117	0.0847	0.0012	0.0024
	Agriculture	0.2352	**0.7130**	0.0105	0.0412	0.3183	0.6215	0.0126	0.0476
	Water	0.1629	0.4530	**0.2659**	0.1182	0.2369	0.4892	0.1588	0.1151
	Vegetation	0.0549	0.3886	0.0671	**0.4894**	0.1153	0.4580	0.0632	0.3634

Table 5. Transition probability matrices of Markov Chain and LCM models (1990–2024).

This contribution has been peer-reviewed. The double-blind peer-review was conducted on the basis of the full paper.
https://doi.org/10.5194/isprs-annals-X-4-W8-2025-675-2026 | © Author(s) 2026. CC BY 4.0 License.

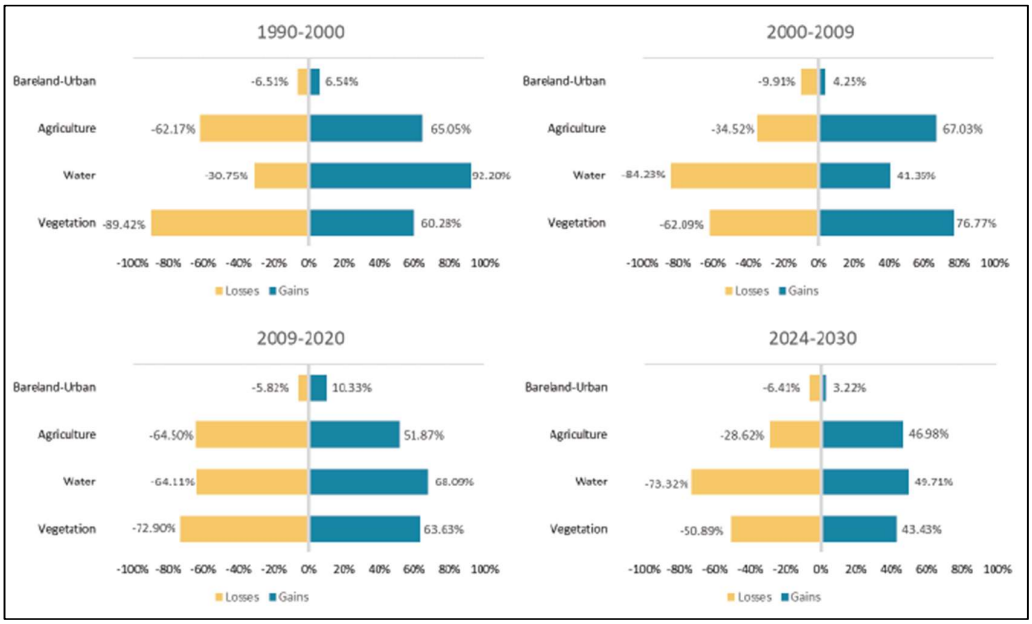

Figure 3- The Gain and Losses of Land use of Shahrekord

Performance of the CA-Markov Prediction Model.The predictive capability of the CA-Markov model was evaluated by comparing its simulated LULC maps for 2020 and 2024 with the corresponding classified reference maps. The results demonstrate that the model performed effectively in reproducing real-world land-use changes across the Shahrekord region. For the 2020 simulation, the model achieved an Overall Accuracy of 80.73%, although some misclassification occurred between the Agriculture (AG) and Built-up/Barren (UB) classes, accounting for a considerable portion of the prediction errors.

Kappa Values	**CA-MARKOV**		**LCM**	
	2020	2024	2020	2024
Kno	0.7851	0.8877	0.8146	0.8911
Kstandard	0.3655	0.5711	0.3641	0.5935

Table 6. Accuracy comparison of different models.

The model's performance improved notably in the 2024 simulation, reaching an Overall Accuracy of 89.75%. The number of mismatched pixels decreased from approximately 239,000 in 2020 to 127,000 in 2024, indicating a much closer alignment between the predicted and actual maps. The CA-Markov model showed strong proficiency in capturing the spatial distribution of the dominant UB and AG classes, successfully reflecting the persistent trends of urban expansion and agricultural adaptation observed in the classified data.Furthermore, the Kappa-based indices (Kno and Kstandard) confirmed this improvement, with higher values obtained for 2024 compared to 2020, reflecting enhanced spatial agreement and reduced random error. Visual inspection of the simulated and actual maps (Figure 3) supports these findings, showing close spatial correspondence across both core urban areas and peripheral agricultural zones. Overall, the strong predictive performance of the CA-Markov model validates its reliability for projecting future land-use scenarios and demonstrates its capability to model complex spatial dynamics within semi-arid urbanizing environments.

6 Discussion

The results of this study demonstrate substantial transformations in land use and land cover within Shahrekord between 1990 and 2024. The consistent increase in urban and bare land, accompanied by a reduction in vegetative cover and fluctuations in agricultural and water areas, highlights a trend toward urban expansion and land conversion. The classification accuracy, particularly from 2000 onwards, remained high, validating the effectiveness of the MLC algorithm and the quality of sample data. The sharp improvement in the Kappa coefficient from 1990 to 2000 (0.382 to 0.790) indicates better representation of class separability with newer satellite sensors and refined training samples. Urban sprawl, as seen by the dominant area of Class 1, has reshaped the spatial configuration of the region. Between 1990 and 2024, urban land area increased slightly overall, though it experienced a small decline from 2020 to 2024. Simultaneously, agricultural land displayed fluctuating trends, with notable recovery between 2009 and 2024. Vegetation and water bodies decreased consistently across the years, likely due to droughts, reduced water availability, and land development pressures. The CA-Markov model proved capable of accurately predicting LULC transitions, especially for the 2024 simulation model performance. Misclassifications, particularly among agriculture and vegetation classes, indicate areas for improvement, possibly through finer classification schemes or incorporation of ancillary data (e.g., elevation, soil type). Overall, these findings underscore the importance of continuous LULC

LULC Classes	Refrence LULC		CA-MARKOV		LCM	
	2020	2024	2020	2024	2020	2024
Bareland-Urban	817.7436	790.8804	817.7436	835.3528	817.7436	826.9279
Agriculture	97.8274	131.7360	97.8274	93.8491	97.8274	97.4473
Water	10.4609	5.4715	10.4609	10.1853	10.4609	9.7017
Vegetation	15.7866	13.7307	15.7866	15.0603	15.7866	20.3707

Table 7 - Distribution of surfaces by models in Km^2.

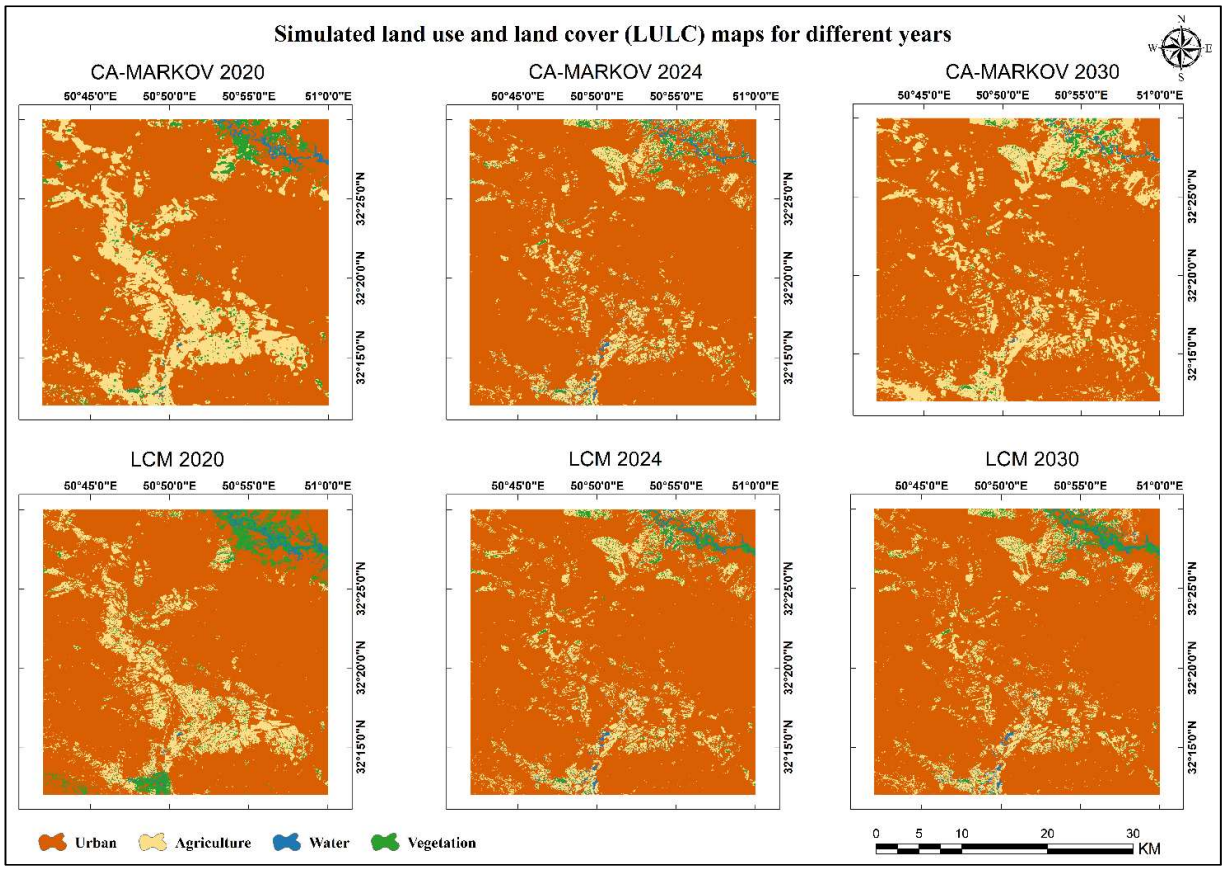

Figure 4 - The overall methodological workflow, from data acquisition in GEE to the final 2030 LULC projection.

monitoring and suggest that modeling approaches like CA-Markov are reliable tools for forecasting land cover dynamics in semi-arid urban regions.

LULC Classes	CA-MARKOV	LCM
	2030	2030
Bareland-Urban	765.6316	813.7546
Agriculture	157.9966	94.6720
Water	4.2862	8.7482
Vegetation	13.8665	24.6062

Table 8 - Distribution of surfaces by models in Km^2.

7. Conclusions

This study successfully integrated remote sensing data, supervised classification, and predictive modeling to monitor and forecast land-use/land-cover (LULC) changes in Shahrekord, Iran. The results revealed a dynamic and rapidly evolving landscape characterized by continuous urban expansion, fluctuating agricultural areas, and a gradual decline in vegetation and water resources. The application of the Maximum Likelihood Classification (MLC) method produced high thematic accuracy, particularly from 2000 onward, confirming the reliability of the sampling design and the effectiveness of the preprocessing workflow. The CA-Markov model demonstrated strong predictive capability, achieving nearly 90% accuracy for the 2024 simulation and accurately replicating the spatial patterns of change observed in the classified maps. This high level of agreement validates the model's suitability for forecasting complex LULC transitions in semi-arid regions experiencing accelerated urbanization. The findings underscore the need for continuous and systematic LULC monitoring using high-resolution and up-to-date satellite data to effectively track urban expansion and environmental degradation. Future modeling efforts should incorporate additional explanatory variables such as topography, socioeconomic indicators, and climate factors to improve predictive accuracy. Furthermore, integrating LULC change predictions into urban and regional planning frameworks can support more sustainable land use and resource management. Particular attention should also be given to the restoration and protection of vegetation and water resources, which are increasingly vulnerable to anthropogenic pressures and climate variability. In summary, the methodological framework developed in this study provides a robust and replicable approach for analyzing and projecting LULC dynamics in urban and semi-arid environments. The outcomes contribute valuable insights into the processes shaping landscape transformation and offer a practical foundation for evidence-based decision-making and sustainable land management in rapidly developing regions.

References

Aburas, M.M., Abdullah, S.H., Ramli, M.F., Ash'aari, Z.H., 2018. Simulating and monitoring future land-use trends using CA–Markov and LCM models. *IOP Conference Series: Earth and Environmental Science*, 169, 012050. https://doi.org/10.1088/1755-1315/169/1/012050

Ait El Haj, F., Ouadif, L., Akhssas, A., 2023. Simulating and predicting future land-use/land-cover trends using CA–Markov and LCM models: Case study of the Lakhdar sub-basin, Morocco. *Case Studies in Chemical and Environmental Engineering*, **7**, 100342. https://doi.org/10.1016/j.cscee.2023.100342

Eastman, J.R., 2016. *TerrSet Geospatial Monitoring and Modeling System (User Manual).* Clark Labs, Clark University, Worcester, MA.

Gorelick, N., Hancher, M., Dixon, M., Ilyushchenko, S., Thau, D., Moore, R., 2017. Google Earth Engine: Planetary-scale geospatial analysis for everyone. *Remote Sensing of Environment*, **202**, 18–27. https://doi.org/10.1016/j.rse.2017.06.031

Richards, J.A., Jia, X., 2006. *Remote Sensing Digital Image Analysis: An Introduction* (4th ed.). Springer, Berlin/Heidelberg. https://doi.org/10.1007/3-540-29711-1

Wang, S.W., Munkhnasan, L., Lee, W.K., 2021. Land use and land cover change detection and prediction in Bhutan's high-altitude city of Thimphu, using cellular automata and Markov chain. *Environmental Challenges*, **2**, 100017. https://doi.org/10.1016/j.envc.2020.100017